

Supporting Information

Oxygen defect based Cobalt-doped-NiMoO₄ Hierarchical hollow nanosheet-based-nanosphere for oxygen evolution reaction

Zhuoxun Yin,^{*,a} Min Zhou,^a Xiping Li,^a Xiangcun Liu,^a Xinzhi Ma,^{*,b} Yang Zhou,^{*,c} Wei Chen,^a Jinlong Li,^a Lina Liu,^a Jun Lv^a

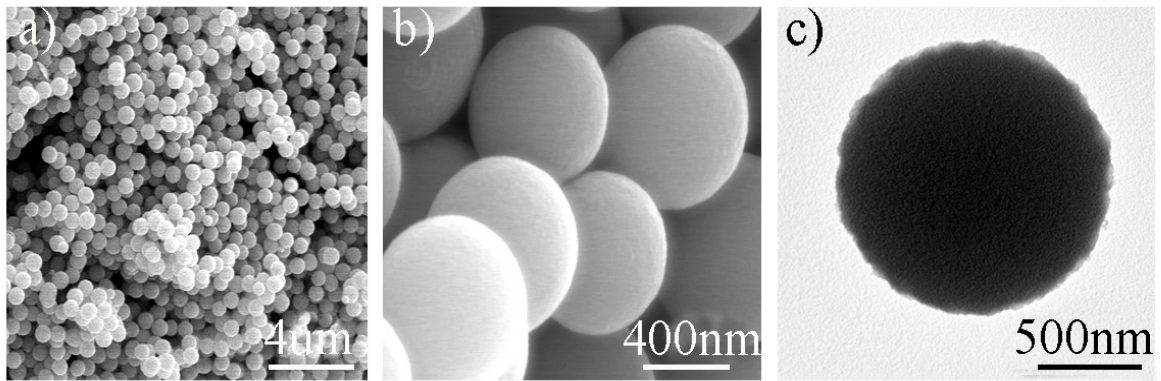


Figure S1 a,b)SEM image of MoEG c) TEM image of MoEG.

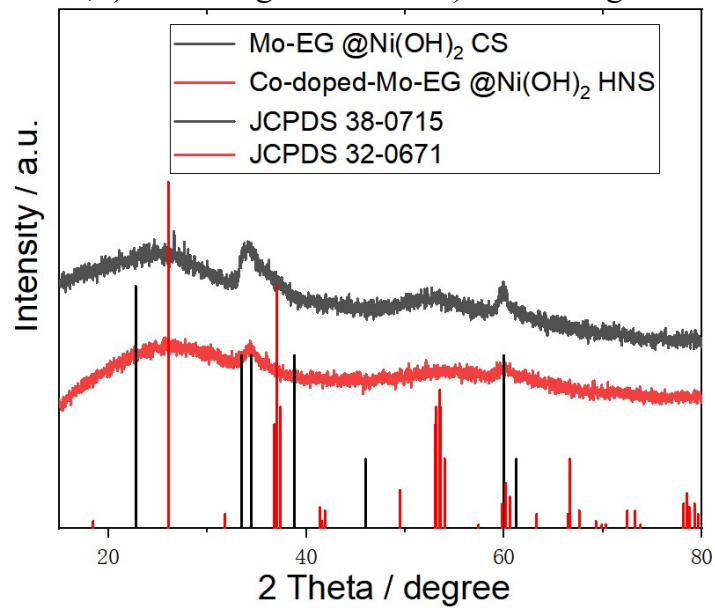


Figure S2 XRD patterns of Mo-EG @Ni(OH)₂ CS and Co-doped-Mo-EG @Ni(OH)₂ HNS

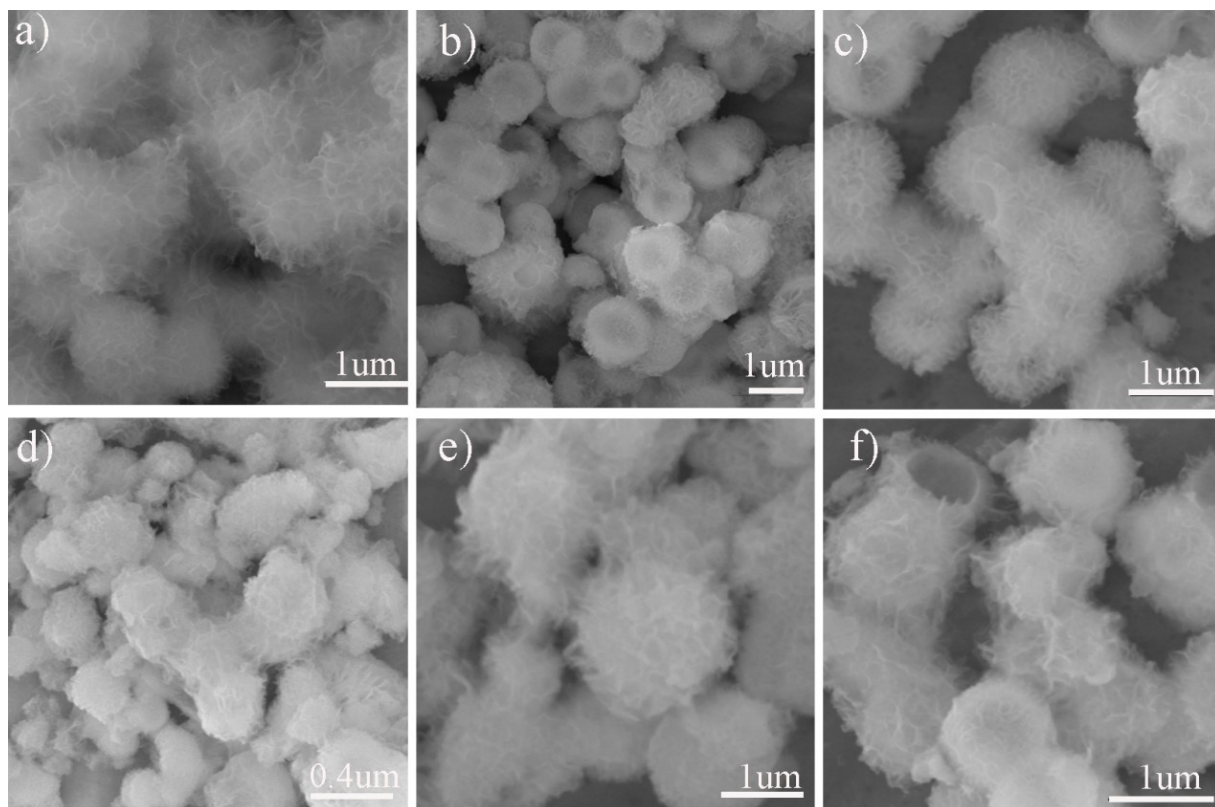


Figure S3 SEM images of the powder samples prepared at a) NiMo-EG b) Co₁-NiMo₄-HNS, c)Co_{1.5}-NiMo₄-HNS, d) Co₂-NiMo₄-HNS, e) Co₄-NiMo₄-HNS, and f)Co₆-NiMo₄-HNS.

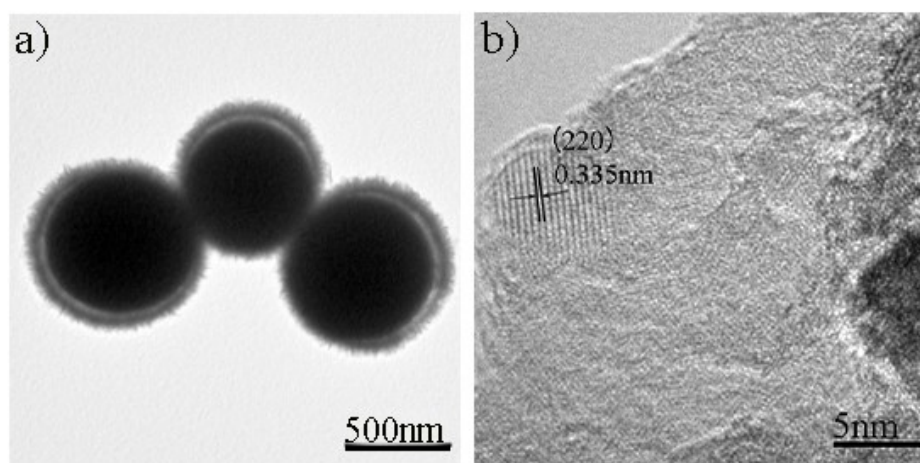


Figure S4 TEM images of NiMoO₄-CS catalysts. a) Low-magnification TEM image, and b) HRTEM image. shows the interplanar distances at marked regions.

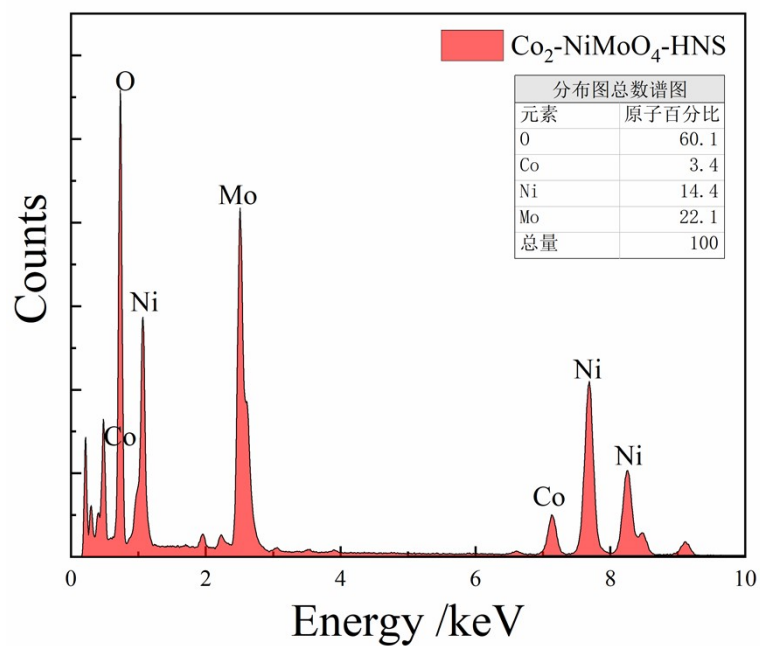


Figure S5 The EDX pattern of the Co₂-NiMoO₄-HNS.

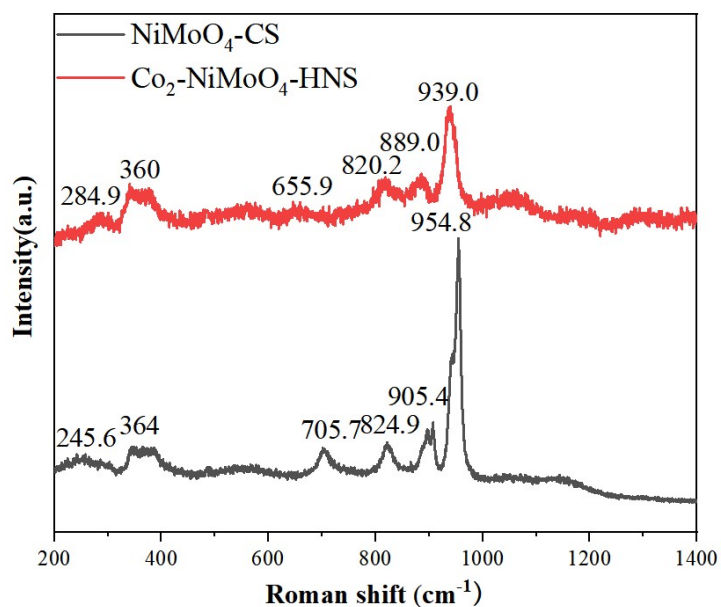


Figure S6 Raman spectra of NiMoO₄ (black) and Co₂-NiMoO₄-HNS (red).

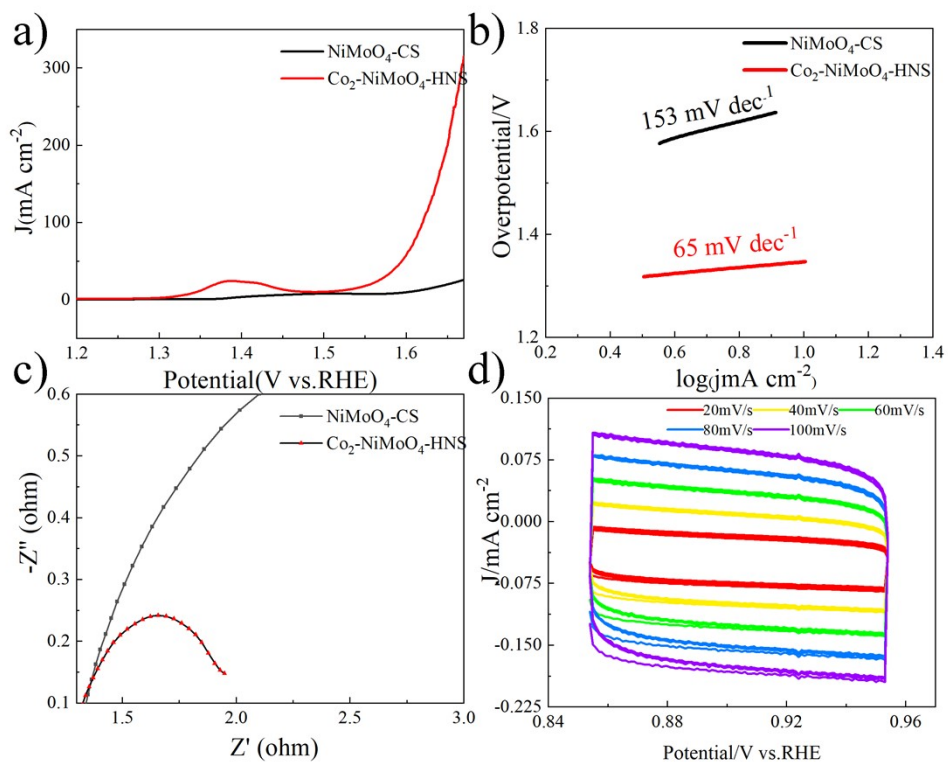


Figure S7 a) The OER polarization curves of $\text{Co}_2\text{-NiMoO}_4\text{-HNS}$ and $\text{NiMoO}_4\text{-CS}$ in 1.0 M KOH. b) The corresponding Tafel plots of $\text{Co}_2\text{-NiMoO}_4\text{-HNS}$ and $\text{NiMoO}_4\text{-CS}$ c) Nyquist plot representations of the electrochemical impedance spectra of $\text{Co}_2\text{-NiMoO}_4\text{-HNS}$ and $\text{NiMoO}_4\text{-CS}$. d) The CV curves of $\text{Co}_2\text{-NiMoO}_4\text{-HNS}$.

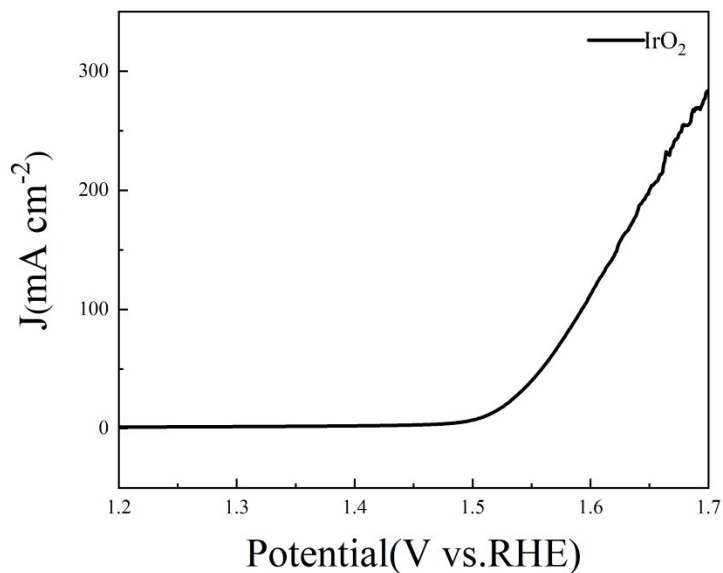


Figure S8 The OER polarization curves of IrO_2 .

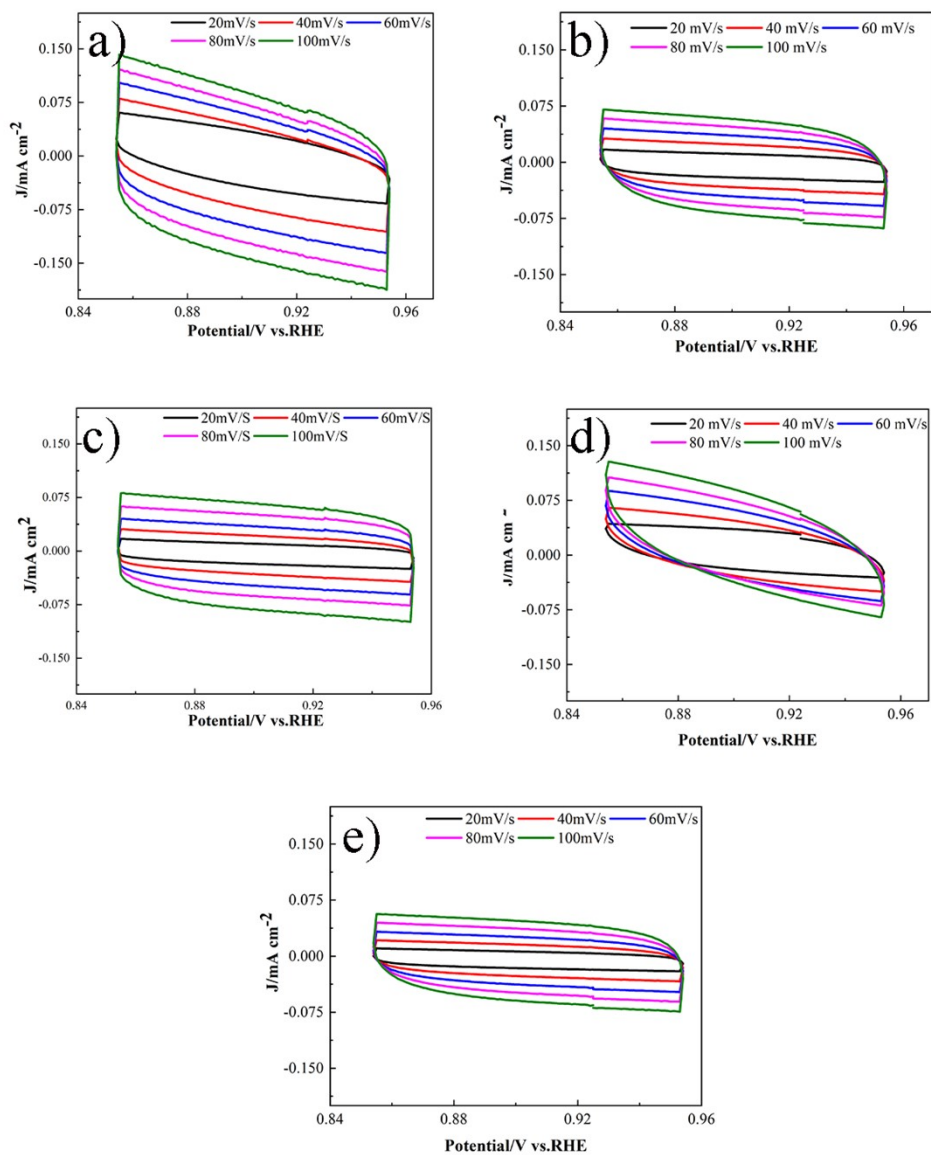


Figure S9 The CV curves of a) $\text{Co}_1\text{-NiMoO}_4\text{-HNS}$, b) $\text{Co}_{1.5}\text{-NiMoO}_4\text{-HNS}$, c) $\text{Co}_2\text{-NiMoO}_4\text{-HNS}$, d) $\text{Co}_4\text{-NiMoO}_4\text{-HNS}$, (e) $\text{Co}_6\text{-NiMoO}_4\text{-HNS}$.

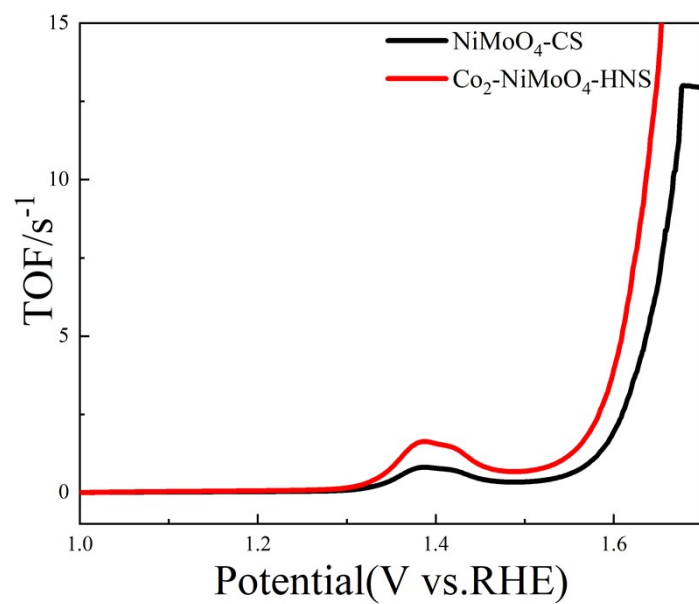


Figure S10 TOF of $\text{Co}_2\text{-NiMoO}_4\text{-HNS}$ and $\text{NiMoO}_4\text{-CS}$.

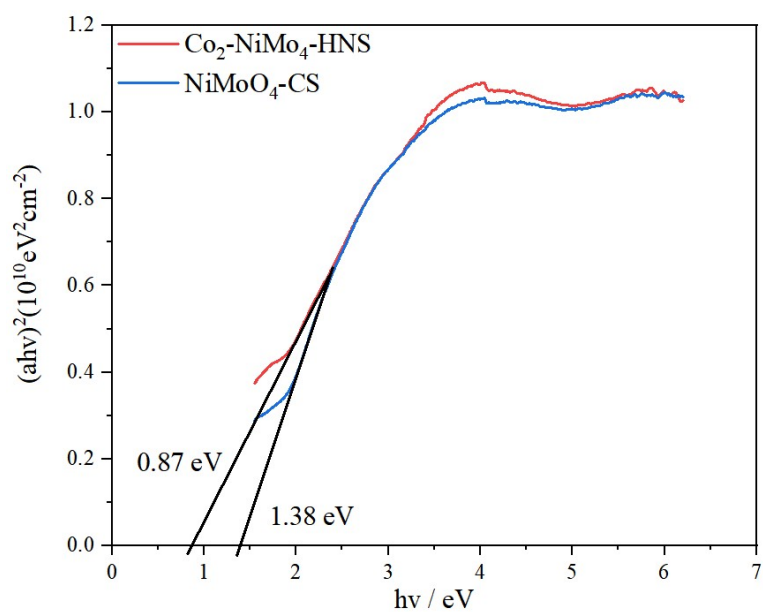


Figure S11 The Kubelka-Munk plot for band gap energy of $\text{Co}_2\text{-NiMoO}_4\text{-HNS}$ and $\text{NiMoO}_4\text{-CS}$

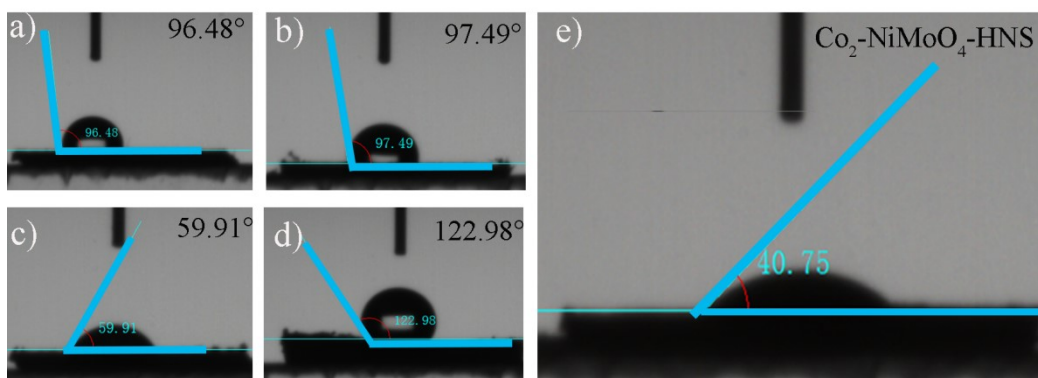


Figure S12 Water contact angle images of a) $\text{Co}_1\text{-NiMoO}_4\text{-HNS}$, b) $\text{Co}_2\text{-NiMoO}_4\text{-HNS}$, c) $\text{Co}_4\text{-NiMoO}_4\text{-HNS}$, d) $\text{Co}_6\text{-NiMoO}_4\text{-HNS}$, e) $\text{Co}_{1.5}\text{-NiMoO}_4\text{-HNS}$.

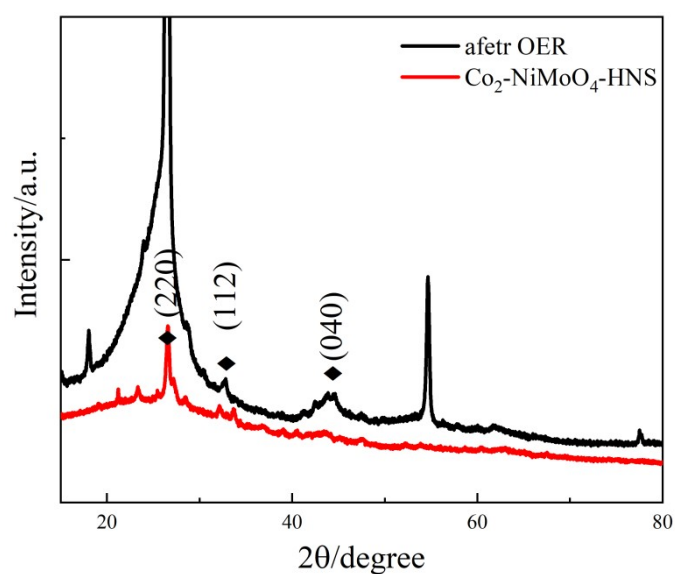


Figure S13 XRD patterns of $\text{Co}_2\text{-NiMoO}_4$ and after OER.

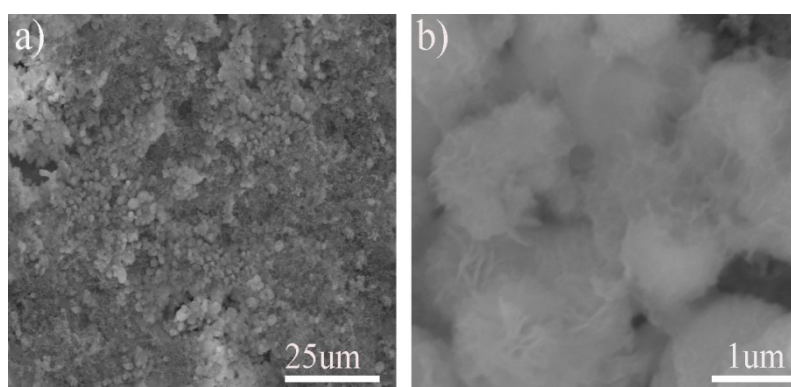


Figure S14 SEM of $\text{Co}_2\text{-NiMoO}_4\text{-HNS}$ after OER.

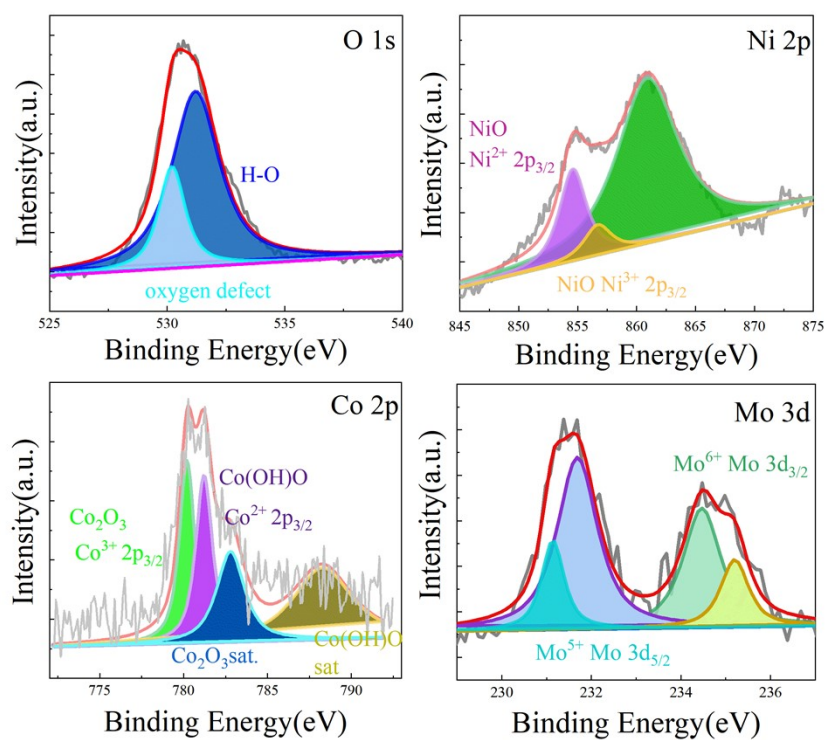


Figure S15 a) high-resolution O 1s XPS spectra for Co₂-NiMoO₄-HNS after OER b) high-resolution Ni 2p XPS spectra for Co₂-NiMoO₄-HNS c) Co 2p d) Mo 3d.

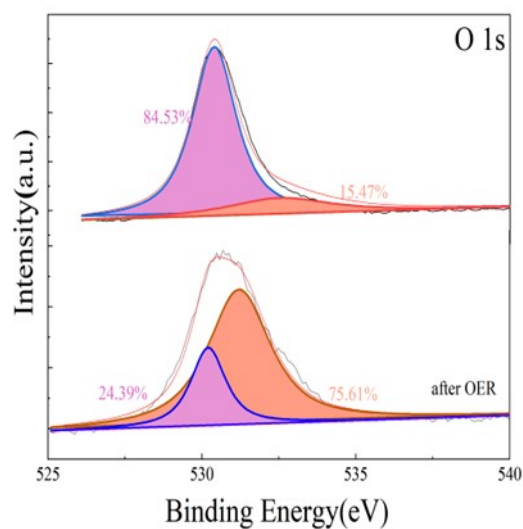


Figure S16 High-resolution XPS spectra of O 1s

Table S1. Comparison of OER activity data among different catalysts.

Catalysts	Overpotential at 10 mA cm⁻² (mV vs RHE)	Electrolyte concentration (pH)	Ref.
Co₂-NiMoO₄-HNS	270	14	This work
Ni_{0.69}Co_{0.31}-P	276	13	1
CoOx-(a)	390	14	2
NiO	420	14	2
NiCoOx	380	14	2
NiMoN-550	312	14	3
Ni₃FeN	280	14	4
Co/N-C-800	274	14	5
Ni10-CoPi	320	14	5
Co₂Fe-MOF	280	14	5
Mn-NiMoO₄	330	14	6
Co₃O₄@NiMoO₄	>300	14	7
NiO@MoO₃/VC	280	14	8
NiMoP@CoCH/CC-2	>270	14	9
NiMn LDHs	350	14	10
Co-NiMoN NRs	294	14	11
Mo₂C@NC/Co@NG-900	420	14	12
Co@Co₃O₄/NC-1	410	14	13

- [1] Yin, Z., Zhu, C., Li, C., Zhang, S., Zhang, X., & Chen, Y. (2016). Hierarchical nickel – cobalt phosphide yolk – shell spheres as highly active and stable bifunctional electrocatalysts for overall water splitting. *Nanoscale*, 8(45), 19129 – 19138. doi:10.1039/c6nr07009d
- [2] C. C. L. McCrory, S. Jung, J. C. Peters and T. F. Jaramillo, *J. Am. Chem. Soc.*, 2013, 135, 16977.
- [3] Z. X. Yin, Y. Sun, C. L. Zhu, C. Y. Li, X. T. Zhang, Y. J. Chen, *J. Mater. Chem. A* 2017, 5, 13648.
- [4] X. D. Jia, Y. F. Zhao, G. B. Chen, L. Shang, R. Shi, X. F. Kang, G. I. N. Waterhouse, L. Z. Wu, C. H. Tung, T. R. Zhang, *Adv. Energy Mater.* 2016, 6, 1502585.
- [5] Xi-Zheng Fan, Xin Du. In Situ Construction of Bifunctional N-Doped Carbon-Anchored Co Nanoparticles for OER and ORR *ACS Appl. Mater. Interfaces*, 2022, 14, 6, 8549 – 8556
- [6] Zhuoxun, Zhang, Chen, etc. Hybrid-atom-doped NiMoO₄ nanotubes for oxygen evolution reaction.
- [7] X. Q. Du, N. Li and X. S. Zhang, *Dalton Trans.*, 2018, 47, 12071.
- [8] R. Illathvalappil, L. George and S. Kurungot, *ACS Appl. Energy Mater.*, 2019, 2, 4987.
- [9] F. F. Wang, K. Ma, W. Tian, J. C. Dong, H. Han, H. P. Wang, K. Deng, H. R. Yue, Y. X. Zhang, W. Jiang and J. Y. Ji, *J. Mater. Chem. A*, 2019, 7, 19589.
- [10] A. Sumboja, J. W. Chen, Y. Zong, P. S. Lee and Z. L. Liu, *Nanoscale*, 2017, 9, 774.
- [11] Z. X. Yin, Y. Sun, Y. J. Jiang, F. Yan and C. L. Zhu, *ACS Appl. Mater. Interfaces*, 2019, 11, 27751.
- [12] Y. Wang, K. Y. Li, F. Yan, C. Y. Li, C. L. Zhu, X. T. Zhang and Y. J. Chen, *Nanoscale*, 2019, 11, 12563.
- [13] A. Aijaz, J. Masa, C. Rçsler, W. Xia, P. Weide, A. J. R. Botz, R. A. Fischer, W. Schuhmann and M. Muhler, *Angew. Chem., Int. Ed.*, 2016, 55, 4087.